Orientation dependence of nonadiabatic molecular high-order-harmonic generation from resonant polar molecules

Xue-Bin Bian* and André D. Bandrauk†
Département de Chimie, Université de Sherbrooke, Sherbrooke, Quebéc J1K 2R1, Canada
(Received 18 September 2012; published 26 November 2012)

Orientation-dependent nonadiabatic molecular high-order-harmonic generation (MHOHG) is studied for the one-electron polar diatomic molecular ion HeH^{2+} exposed to short, linearly polarized, intense laser fields. The fully dimensional time-dependent Schrödinger equation is solved numerically. The resonance of excited states is maximal in the parallel orientation, while it is minimal in the perpendicular case for the nonsymmetric molecular ion. The resulting redshift and the overall intensity of MHOHG strongly depend on the electronic symmetry and charge transfer of the resonant excited states. These results are used to confirm the proposed four-step model in MHOHG involving intermediate resonance states.

DOI: 10.1103/PhysRevA.86.053417 PACS number(s): 33.80.Rv, 42.65.Ky, 34.50.Gb

I. INTRODUCTION

High-order-harmonic generation (HHG) is a nonlinear process to generate coherent attosecond (1 as $= 10^{-18}$ s) laser pulses [1]. It has received a lot of attention recently [2–5], as it provides an important tabletop XUV source to investigate ultrafast electronic dynamics [6]. The general feature of HHG spectra from strong laser-gas interaction is the rapid decay of lower order harmonics, followed by a long plateau, and the short cutoff with a photon energy around $I_p + 3.17U_p$ (where I_p is the ionization potential, and $U_p = I/4\omega^2$ denotes the ponderomotive energy). A semiclassical three-step model has been used successfully to interpret the HHG mechanism for initial zero-velocity ionized electrons [7] and nonzero-velocity electrons [8]. In this model, when atoms and molecules are exposed to intense laser fields, the electron is initially ionized by tunneling from the ground state. It is then accelerated by the laser field and returns to the original ion to recombine with the parent ion and emit HHG photons due to a phase change of the electric field. This model successfully explains the maximum cutoff energy $I_p + 3.17U_p$ of HHG observed in atoms and molecules [5]. However, this model neglects the structure of molecules and the role of excited states in HHG.

Due to permanent dipoles, polar molecules have received increasing attention recently [9–13]. The phenomena of enhanced excitation and enhanced ionization have been reported [9] to be essential phenomena in molecules. Harmonics with cutoff energies higher than $I_p + 3.17U_p$ can be obtained in laser-induced electron transfer with the neighboring ions [14–17] in molecules and is called MHOHG, molecular high-order-harmonic generation. In our previous work, we proposed a four-step model [17,18] to interpret multichannel MHOHG in resonant dipolar molecular systems. The electron in the ground state is pre-excited to a localized resonant excited state with a long lifetime [19] first, then it is ionized and oscillates in the laser fields, acquiring kinetic energy. Finally, it recombines with the ground state and emits high-energy photons. MHOHG for such resonant systems can be described by the above four-step model and has novel features, which do not occur in the three-step model of atomic HHG. For example, resonance-enhanced-harmonic generation, multiple-frequency harmonic series, double plateaus, a higher cutoff energy [10,17], and nonadiabiatic redshift of MHOHG [18] are predicted by this model. In particular, a time delay between enhanced excitation and subsequent enhanced ionization has been shown to produce a noticeable "redshift" in MHOHG for very short pulses [18].

In this paper, we study the orientation [20–22] dependence of resonant MHOHG in linearly polarized laser fields for the one-electron polar molecular ion HeH^{2+}. The rest of this paper is organized as follows. The numerical method is presented in Sec. II. The results and discussion are in Sec. III. The conclusion of the paper is given in Sec. IV.

II. THEORETICAL METHOD

For diatomic molecular systems, prolate spheroidal coordinates are accurate to deal with the nuclear potential terms [17]. If the internuclear distance R is small, spherical coordinates are also a good choice with a satisfactory precision [23]. In this paper, we adopt the latter coordinates since this method is easy to generalize in molecular systems with multiple centers [24].

The field-free Hamiltonian in the Born-Oppenheimer approximation is (atomic units are used throughout; $e = \hbar = m_e = 1$)

$$H_0 = -\frac{1}{2}\nabla^2 - \frac{Z_2}{|\mathbf{r} + \mathbf{R}/2|} - \frac{Z_1}{|\mathbf{r} - \mathbf{R}/2|}, \tag{1}$$

where R is the nuclear distance, and Z_1 and Z_2 are nuclear charges, respectively. A multipole expansion of the nuclear attraction potential gives [24]

$$\frac{1}{|\mathbf{r} - \mathbf{R}/2|} = \sum_{\lambda=0}^{\infty} \frac{r_<^\lambda}{r_>^{\lambda+1}} P_\lambda(\cos\theta). \tag{2}$$

Here $r_<$ ($r_>$) is the smaller (larger) one of the r and $R/2$, and $P_\lambda(\cos\theta)$ are the Legendre polynomials.

The wave function is expanded by B splines [24]:

$$\Psi(r,\xi,\phi) = \sum_{i,j,m} C_{i,j}^m B_i(r)(1-\xi^2)^{\frac{|m|}{2}} B_j(\xi)\frac{\exp(im\phi)}{\sqrt{2\pi}}, \tag{3}$$

with $\xi = \cos\theta$.

*xue.bin.bian@usherbrooke.ca
†andre.bandrauk@usherbrooke.ca

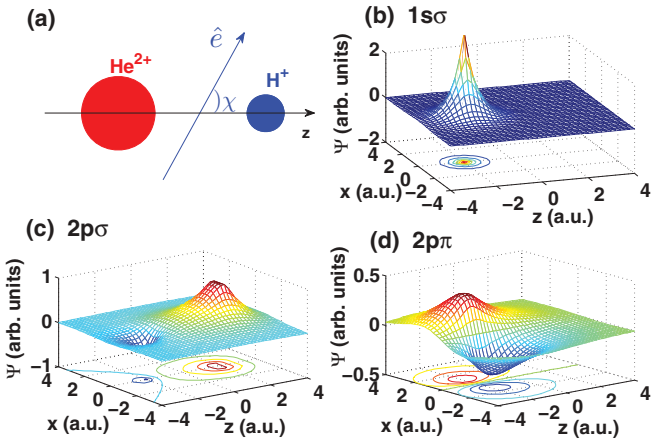

FIG. 1. (Color online) (a) Molecular geometry of HeH^{2+} in linearly polarized laser fields. Wave functions of (b) the $1s\sigma$ state, (c) the $2p\sigma$ state, and (d) the $2p\pi$ state.

The interaction of the system with a linearly polarized laser field is described by the corresponding time-dependent Schrödinger equation as

$$i\frac{\partial}{\partial t}\Psi(\mathbf{r},t) = [H_0 + H(t)]\Psi(\mathbf{r},t), \tag{4}$$

where the interaction term in length gauge is $H(t) = \mathbf{E}(t)\cdot\mathbf{r}$. We set the molecular axis along the z axis, and the laser polarization has a fixed angle χ with the molecular axis in the xz plane as illustrated in Fig. 1(a). The interaction term can then be written as $H(t) = E(t)(z\cos\chi + x\sin\chi)$. The electric field of the laser pulse is given by $\mathbf{E}(t) = E_0 f(t)\cos(\omega t)\hat{\mathbf{e}}$, $t\in[-\tau/2,\tau/2]$, with the pulse shape $f(t) = \cos^2(\pi t/\tau)$, where τ is the total duration of the laser pulses.

The time propagation scheme used in this paper is the Crank-Nicolson method, which expresses the exponential operator to the third order as

$$\exp(-iH\Delta t) = \frac{1 - iH\Delta t/2}{1 + iH\Delta t/2} + O(\Delta t^3). \tag{5}$$

We have built an efficient parallel code to solve the above full-dimensional time-dependent Schrödinger equation. After obtaining numerically the wave function $\Psi(\mathbf{r},t)$ at any time t, the power spectra of MHOHG are calculated by Fourier transformation of the dipole momentum in acceleration form $d_A(t)$. $d_A(t)$ is obtained by the Ehrenfest theorem [22]:

$$d_A(t) = \langle\Psi(\mathbf{r},t)|\hat{\mathbf{e}}\cdot[\nabla V(r) + \mathbf{E}(t)]|\Psi(\mathbf{r},t)\rangle. \tag{6}$$

This is the most reliable numerical method for strong-field interactions, thus avoiding transient effects in very short pulses due to nonrecolliding electrons [25]. To reduce the reflection from the boundary, a $\cos^{1/8}$ mask function is used at every time step [17].

To further probe the temporal structures of MHOHG, we perform a time profile analysis of the harmonic spectra. The time profile of harmonic ω_q is obtained by a wavelet analysis [26,27],

$$d(\omega_q,t) = \int d_A(t) w_{t,\omega_q}(t')dt', \tag{7}$$

with the wavelet kernel $w_{t,\omega_q}(t') = \sqrt{\omega_q}W(\omega_q(t'-t))$. The mother wavelet we use is a Morlet wavelet:

$$W(x) = (1/\sqrt{\sigma})e^{ix}e^{-x^2/2\sigma^2}. \tag{8}$$

III. RESULTS AND DISCUSSION

In this paper, the peak intensity of the laser field is $I = 3.5\times10^{15}$ W/cm^2, the wavelength is $\lambda = 400$ nm, and the duration of the laser pulse is $\tau = 15$ optical cycles. The internuclear distance is fixed at $R = 4$ a.u. (near the excited-state minimum $R = 3.89$ a.u.). The convergence of the numerical calculations in this work is achieved by varying the number of basis vectors and time steps. The wave function in Eq. (3) is expanded by 350 B splines in the radial direction and 36 B splines in the angular ξ direction. The quantum number m is truncated with $|M\text{max}| = 20$. Four thousand ninety-six time steps per optical cycle are used in the time propagation. To obtain the initial state, an imaginary time propagation method ($t\to -it$) is used. The obtained energies of the ground state $1s\sigma$ and the excited states $2p\sigma$ and $2p\pi$ are -2.2506, -1.0310, and -0.7388 a.u., respectively, which agree well with recent results reported in the literature [28]. The corresponding wave functions Ψ are also illustrated in Fig. 1. For the $1s\sigma$ state, the wave function is concentrated on He^{2+}, while for the $2p\sigma$ state the corresponding wave function has a larger portion on H^+. As a result, the transition between the $1s\sigma$ and the $2p\sigma$ states corresponds to a charge transfer from one core to the other for parallel orientation [17]. The $2p\pi$ state is excited for a perpendicular orientation. Its wave function remains concentrated on He^{2+} and is antisymmetric with respect to the yz plane. In our numerical simulations, the initial state is the ground state. The MHOHG spectra with different orientation angles χ and the corresponding time profiles obtained by wavelet analysis are shown in Figs. 2 to 6.

A. Intensity dependence of MHOHG on the resonance of excited states

In Figs. 2 to 6, one can see that the overall intensity of MHOHG is strongly dependent on the resonance of the excited states. The intensity of MHOHG in the plateau for a parallel orientation $\chi = 0^\circ$ is more than two orders higher than that with $\chi = 90^\circ$ for a perpendicular orientation. The reason is that the ionization rate from the excited state $2p\sigma$ is around seven orders higher than that from the ground state under the current laser conditions [17]. A small population in the excited state $2p\sigma$ greatly enhances the ionization rate. For the parallel orientation, the amplitude of transition to the $2p\sigma$ state, which is a localized state on H^+, is maximal. This corresponds to an efficient laser-induced electron transfer in a nonsymmetric system. One can observe a strong resonance in the MHOHG spectra in Fig. 2(a). The position of the resonance at around harmonic order 18 agrees well with the energy difference between the dressed $1s\sigma$ and $2p\sigma$ states [17]. This resonance can also be seen in the time profile of MHOHG in Fig. 2(b). When we gradually increase the orientation angle χ between the laser polarization and the molecule axis, the intensity of the resonance and overall MHOHG decreases as illustrated in Figs. 3 to 6. When $\chi > 45^\circ$, no obvious resonance is observed

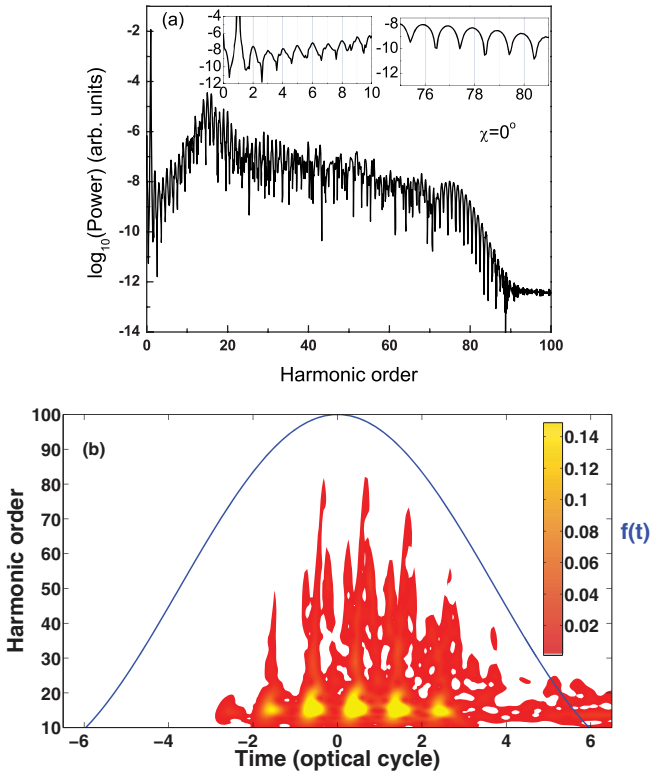

FIG. 2. (Color online) (a) MHOHG spectra of HeH^{2+} in linearly polarized laser fields and (b) wavelet analysis of the harmonic generation. Inset in (a): The enlarged area of MHOHG. The internuclear distance $R = 4$ a.u. is fixed. The initial state is the ground state $1s\sigma$. The laser polarization is along the z axis, i.e., $\chi = 0°$. The peak laser intensity is $I = 3.5 \times 10^{15}$ W/cm^2. The wavelength is 400 nm. The pulse has a cos^2 shape with a duration of 15 optical cycles as illustrated in (b).

in the MHOHG spectra or the corresponding time-profile analysis. For a perpendicular orientation with $\chi = 90°$, the amplitude of the transition from $1s\sigma$ to $2p\sigma$ is 0. The resonance in MHOHG is negligible. Consequently, the total ionization rate of the system is lower, and the intensity of the MHOHG in the plateau is two orders lower than that with $\chi = 0°$. These results show that the resonance of the excited state strongly influences the harmonic intensity.

B. Intensity modulation of even and odd MHOHG with different orientation angles

The presence of odd and even harmonics reflects the symmetry of a system. For symmetric systems such as H_2^+, the three-step or four-step model predicts the same recombination dynamics every half-cycle $T_0/2$. In the frequency domain, the frequency difference between each harmonic is 2ω, so that only odd harmonics appear in the spectra of symmetric systems. However, for asymmetric systems, the harmonic generation process repeats itself at every cycle T_0 due to the lack of symmetry, and the frequency interval of harmonics is ω. Both even and odd harmonics appear in the harmonic spectra [29]. For the HeH^{2+} molecular ion as shown in Fig. 1, which has rotational symmetry along the z axis, the asymmetry is maximal with respect to the xy plane. Intuitively, when we

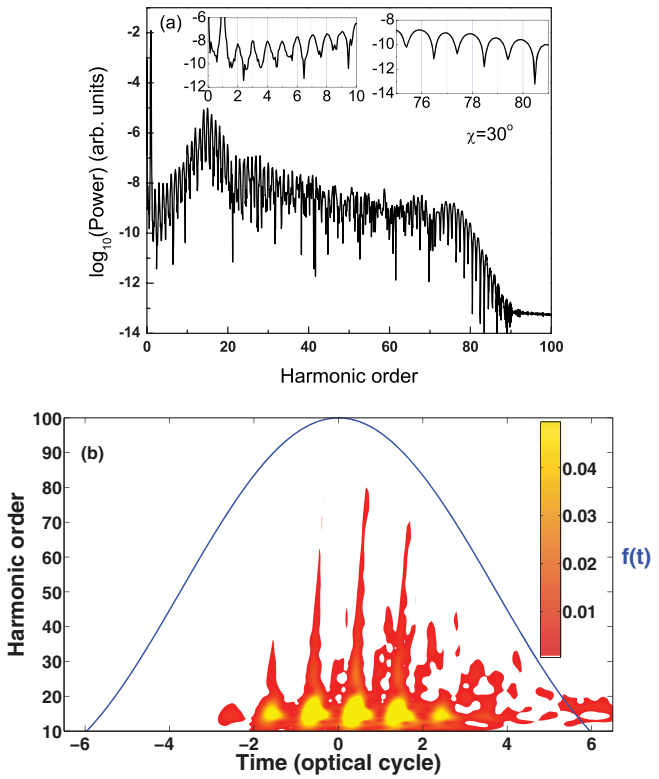

FIG. 3. (Color online) The same as Fig. 2 but with $\chi = 30°$.

gradually increase the laser-molecule orientation angle χ, the relative intensity between odd and even harmonics will increase. When $\chi = 90°$, even harmonics should disappear

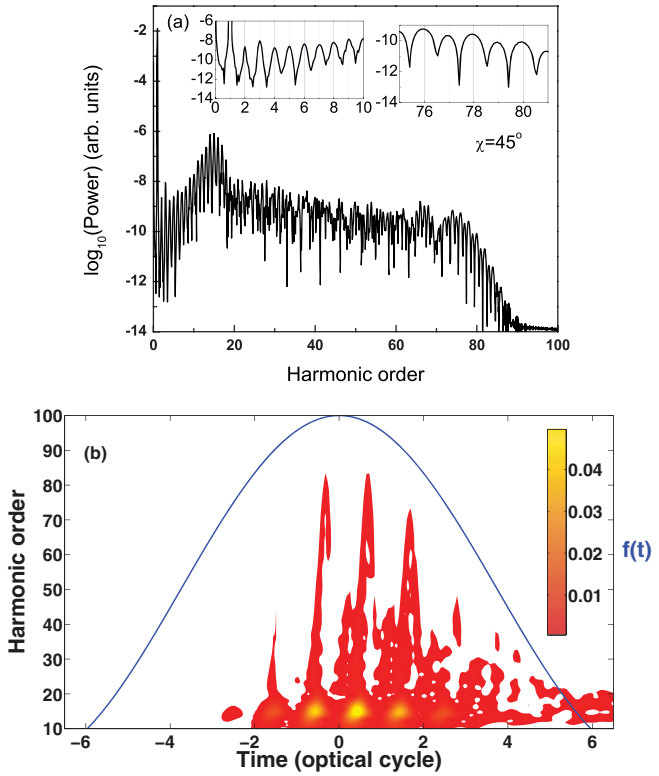

FIG. 4. (Color online) The same as Fig. 2, but with $\chi = 45°$.

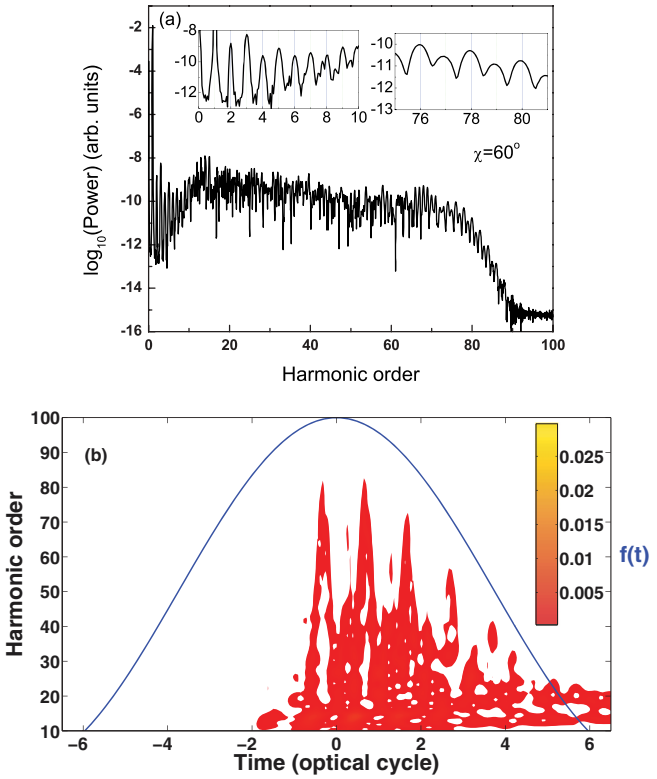

FIG. 5. (Color online) The same as Fig. 2, but with $\chi = 60°$.

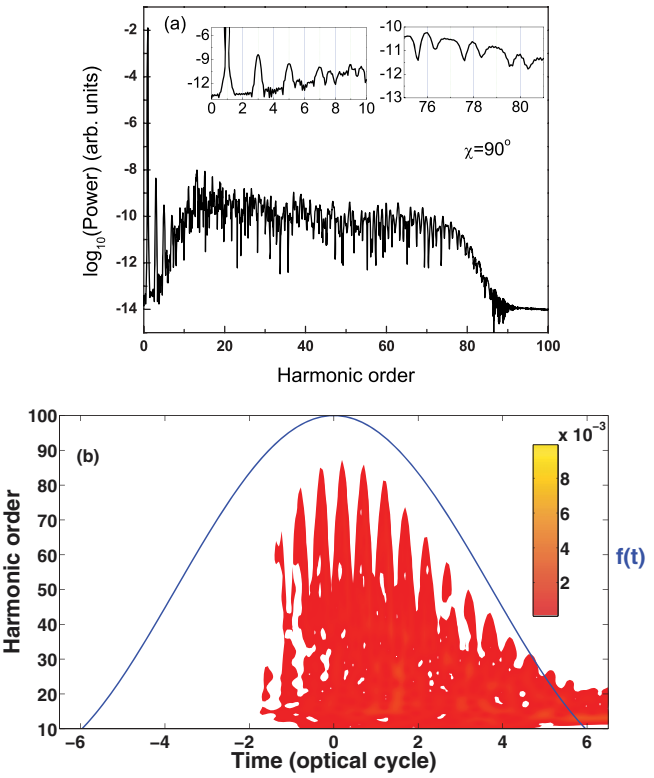

FIG. 6. (Color online) The same as Fig. 2, but with $\chi = 90°$.

owing to the symmetry with respect to the yz plane. However, the harmonic spectra presented in Figs. 2 to 6 are not simple. The lower (below threshold) and higher (near cutoff) order harmonics areas are enlarged in the figures. The lower-order harmonics behave as expected, but the higher order harmonics are contrary to what is expected. In the vicinity of the cutoff, *even-order* harmonics remain when $\chi = 90°$, and their intensity is higher than that of the neighboring odd harmonics. To interpret these counterintuitive observations, contributions from different states have to be included. Harmonics of order less than 10 are in the perturbative regime. Even though the long trajectory can contribute to harmonics close to the ionization threshold [30–32], its role in the well-below-threshold ionization harmonics is negligible, as they are of a pure molecular bound-state character. The corresponding photon energy of harmonics of order $N < 10$ is lower than the transition energy between the ground state $1s\sigma$ and the first excited state $2p\sigma$. Neither contributions from the excited states nor ionization occurs, so that the above three-step or four-step model fails in this regime. As a consequence, there will not be a nonadiabatic redshift in the harmonic spectra. When $\chi = 90°$, even harmonics disappear in the lower order harmonics due to the symmetry of the ground state. However, for higher order harmonics in the nonperturbative regime, populations in excited states should be included. If we take the excited state $2p\pi$ into account, the asymmetry of the total wave function, a superposition of $1s\sigma$ and $2p\pi$ states, i.e., $\Psi = c_1\Psi_{1s\sigma} + c_2\Psi_{2p\pi}$, increases when we gradually increase c_2. Due to the radiation transition selection rule, $c_2 = 0$ when $\chi = 0°$, while c_2 is maximal when $\chi = 90°$ with maximal transition amplitude in the x direction. Since the harmonics near the cutoff region come from high-energy electrons ionized near the peak of the electric field predicted by the three-step or four-step model, the asymmetry of the superposition of the ground and excited states plays a key role in the harmonic generation. Consequently, near the cutoff, even-order harmonics occur with an intensity higher than that of the neighboring odd-order harmonics.

C. Redshift of MHOHG with different orientation angles

Another important feature in our simulations is the dependence of the *redshift* of harmonics on the orientation angle χ. As presented in Figs. 2 to 6, the redshift of harmonics above the ionization threshold is maximal when $\chi = 0°$, while the shift is negligible when $\chi = 90°$. As explained in our previous work with a four-step model [18], this is due to the nonadiabatic response of the molecular dipole to the rapid change of laser intensity [18,33,34]. On the intensity-increasing part of the laser pulse ($t < 0$), the laser field pumps part of the system from the ground state $1s\sigma$ to the resonant state $2p\sigma$ with a long lifetime. As a consequence, in the falling-intensity part of the laser pulse ($t > 0$) the ionization rate is higher than in the rising part, and most of the harmonics are emitted with a rapidly decreasing laser intensity, $I(t)$, with $t > 0$ for very short pulses. The result of $dI(t)/dt < 0$ is a negative chirp of harmonics. Consequently, the electronic kinetic energies obtained from the laser fields are reduced, which leads to the redshift of the harmonics. When the orientation angle χ increases, the transition probability to the resonant $2p\sigma$ is decreased as the z radiative transition momentum vanishes. When $\chi = 90°$, the direct transition amplitude from the ground state $1s\sigma$ to $2p\sigma$ is 0. The four-step model, which involves

a resonant intermediate state, becomes the simple three-step model, and the ionization rate in the decreasing part of the pulse when $t > 0$ is comparable to that in the rising part with $t < 0$. The blueshift generated in the rising part of the pulse with $dI(t)/dt > 0$ will compensate the redshift produced in the falling part of the pulse. As a result, the overall shift of the harmonics is considerably reduced. This is confirmed by the MHOHG spectra and the corresponding time profile analysis in Fig. 6.

IV. CONCLUSION

We have studied the orientation dependence of nonadiabatic effects in MHOHG from the nonsymmetric HeH^{2+} in short, intense laser pulses. It is shown that the resonance effect of excited states is strongly dependent on the orientation angle χ between the molecular axis and the laser polarization direction. This forcefully influences the intensity of some specific and the overall harmonics. The resulting redshift of harmonics predicted previously [18] also depends on the orientation angle χ. For a parallel orientation, the intensity and redshift of MHOHG are maximal, while they are minimal with a vertical orientation, which agrees well with the proposed four-step model. For a perpendicular orientation, even though the molecular structure of the system is symmetric with respect to the yz plane, even harmonics are produced due to the asymmetry of the electron distribution in the resulting superposition of the ground and excited states.

The present simple HeH^{2+} system emphasizes that the principle of nonadiabatic MHOHG is general, which can be used for other polar molecules, like HCl and CO. The resonance of an intermediate state is the key source of the four-step model in polar molecules. Since resonances in HHG have also been observed experimentally in laser-plasma interaction systems [35–37], we predict that the appearance of a redshift and even-order harmonics should also be observed experimentally in such media.

ACKNOWLEDGMENTS

We thank RQCHP and Compute Canada for access to massively parallel computer clusters.

[1] P. B. Corkum and F. Krausz, Nature Phys. **3**, 381 (2007).
[2] T. Brabec and F. Krausz, Rev. Mod. Phys. **72**, 545 (2000).
[3] H. Niikura, D. M. Villeneuve, and P. B. Corkum, Phys. Rev. Lett. **94**, 083003 (2005).
[4] M. V. Frolov, N. L. Manakov, T. S. Sarantseva, M. Yu. Emelin, M. Yu. Ryabikin, and Anthony F. Starace, Phys. Rev. Lett. **102**, 243901 (2009).
[5] A. D. Bandrauk, S. Barmaki, S. Chelkowski, and G. Lagmago Kamta, in *Progress in Ultrafast Intense Laser Science*, edited by K. Yamanouchi (Springer, New York, 2007), Vol. III.
[6] T. Popmintchev *et al.*, Science **336**, 1287 (2012).
[7] P. B. Corkum, Phys. Rev. Lett. **71**, 1994 (1993).
[8] A. D. Bandrauk, S. Chelkowski, and S. Goudreau, J. Mod. Opt. **52**, 411 (2005).
[9] G. L. Kamta and A. D. Bandrauk, Phys. Rev. Lett. **94**, 203003 (2005).
[10] A. Etches and L. B. Madsen, J. Phys. B **43**, 155602 (2010).
[11] H. Akagi *et al.*, Science **325**, 1364 (2009).
[12] X. J. Li, S. F. Zhao, and X. X. Zhou, Commun. Theor. Phys. **58**, 419 (2012).
[13] Y. J. Chen and B. Zhang, Phys. Rev. A **86**, 023415 (2012).
[14] A. D. Bandrauk, S. Barmaki, and G. L. Kamta, Phys. Rev. Lett. **98**, 013001 (2007).
[15] A. D. Bandrauk, S. Chelkowski, H. Yu, and E. Constant, Phys. Rev. A **56**, R2537 (1997).
[16] P. Moreno, L. Plaja, and L. Roso, Phys. Rev. A **55**, R1593 (1997).
[17] X. B. Bian and A. D. Bandrauk, Phys. Rev. Lett. **105**, 093903 (2010); Phys. Rev. A **83**, 023414 (2011).
[18] X. B. Bian and A. D. Bandrauk, Phys. Rev. A **83**, 041403(R) (2011).
[19] I. Ben-Itzhak, I. Gertner, O. Heber, and B. Rosner, Phys. Rev. Lett. **71**, 1347 (1993).
[20] D. G. Lappas and J. P. Marangos, J. Phys. B **33**, 4679 (2000).
[21] M. Lein, P. P. Corso, J. P. Marangos, and P. L. Knight, Phys. Rev. A **67**, 023819 (2003).
[22] G. L. Kamta and A. D. Bandrauk, Phys. Rev. A **71**, 053407 (2005).
[23] T. K. Kjeldsen, L. A. A. Nikolopoulos, and L. B. Madsen, Phys. Rev. A **75**, 063427 (2007).
[24] X. B. Bian, L. Y. Peng, and T. Y. Shi, Phys. Rev. A **78**, 053408 (2008); **77**, 063415 (2008).
[25] A. D. Bandrauk, S. Chelkowski, D. J. Diestler, J. Manz, and K. J. Yuan, Phys. Rev. A **79**, 023403 (2009).
[26] P. Antoine, B. Piraux, and A. Maquet, Phys. Rev. A **51**, R1750 (1995).
[27] C. Chandre, S. Wiggins, and T. Uzer, Physica D **181**, 171 (2003).
[28] J. A. Campos, D. L. Nascimento, D. T. Cavalcante, A. L. A. Fonseca, and A. O. C. Nunes, Int. J. Quantum Chem. **106**, 2587 (2006).
[29] E. Frumker, C. T. Hebeisen, N. Kajumba, J. B. Bertrand, H. J. Wörner, M. Spanner, D. M. Villeneuve, A. Naumov, and P. B. Corkum, Phys. Rev. Lett. **109**, 113901 (2012).
[30] D. C. Yost, T. R. Schibli, J. Ye, J. L. Tate, J. Hostetter, M. B. Gaarde, and K. J. Schafer, Nat. Phys. **5**, 815 (2009).
[31] E. P. Power, A. M. March, F. Catoire, E. Sistrunk, K. Krushelnick, P. Agostini, and L. F. DiMauro, Nat. Photonics **4**, 352 (2010).
[32] J. A. Hostetter, J. L. Tate, K. J. Schafer, and M. B. Gaarde, Phys. Rev. A **82**, 023401 (2010).
[33] M. Geissler, G. Tempea, and T. Brabec, Phys. Rev. A **62**, 033817 (2000).
[34] I. P. Christov, J. Zhou, J. Peatross, A. Rundquist, M. M. Murnane, and H. C. Kapteyn, Phys. Rev. Lett. **77**, 1743 (1996).
[35] D. B. Milošević, Phys. Rev. A **81**, 023802 (2010).
[36] V. Strelkov, Phys. Rev. Lett. **104**, 123901 (2010).
[37] R. A. Ganeev, M. Suzuki, M. Baba, H. Kuroda, and T. Ozaki, Opt. Lett. **31**, 1699 (2006).